Crystallization Behavior of Amorphous Fe90-XNb10BX (X = 10 and 30) Alloys

Materials Transactions, JIM, Vol. 41, No. 11 (2000) pp. 1526 to 1529
Special Issue on Bulk Amorphous, Nano-Crystalline and Nano-Quasicrystalline Alloys

Crystallization Behavior of Amorphous $Fe_{90-X}Nb_{10}B_X$ (X = 10 and 30) Alloys

Muneyuki Imafuku[1], Shigeo Sato[1], Hisato Koshiba[1,*], Eiichiro Matsubara[2] and Akihisa Inoue[2]

[1]*Inoue Superliquid Glass Project, Exploratory Research for Advanced Technology, Japan Science and Technology Corporation, Sendai 982-0807, Japan*
[2]*Institute for Materials Research, Tohoku University, Sendai 980-8577, Japan*

The phase transformation of $Fe_{90-X}Nb_{10}B_X$ (X = 10 and 30) amorphous alloys by annealing was studied by differential scanning calorimetry (DSC) and X-ray diffraction. The $Fe_{60}Nb_{10}B_{30}$ alloy exhibits a large supercooled liquid region (*i.e.* the difference between the glass transition temperature (T_g) and the onset of crystallization temperature (T_x)), ΔT_x ($=T_x - T_g$) of 67 K, whereas the $Fe_{80}Nb_{10}B_{10}$ amorphous alloy transforms directly into crystalline phases. New metastable crystalline phases were found during the crystallization process of these alloys. In the crystallization process of the $Fe_{80}Nb_{10}B_{10}$ alloy, the structure of the primary precipitation phase is α-Mn type, which transforms into α-Fe phase at a higher temperature. In case of $Fe_{60}Nb_{10}B_{30}$ alloy, another metastable phase, $Fe_{23}B_6$-type structure, is formed corresponding to the first exothermic peak in the DSC curve. Although the metastable phases in the two alloys are completely different, the dissociated phases of α-Fe, Fe_3B and Fe_2B are formed in both alloys after the final stage of crystallization. The local atomic ordering structure in the α-Mn type is similar to that in an amorphous state of the $Fe_{80}Nb_{10}B_{10}$ alloy. On the other hand, the formation of the $Fe_{23}B_6$-type structure requires a significant change in the geometrical rearrangements with relatively long-range ordering of the $Fe_{60}Nb_{10}B_{30}$ alloy, which may be attributed to the high stability of the supercooled liquid.

(Received May 22, 2000; Accepted July 28, 2000)

Keywords: *iron-based amorphous alloy, iron-niobium-boron system, glass transition, crystallization, metastable phase, α-manganese, $Fe_{23}B_6$*

1. Introduction

A number of new metallic glasses with a large supercooled liquid region before crystallization have been found in Mg-,[1] Ln-,[2] Pd-,[3] Zr-,[4] and Fe-based[5] systems in recent years. Among these alloys, Fe-based metallic glasses are specially fascinating for practical applications as a new type of soft magnetic material and have been investigated extensively. For example, soft magnetic bulk amorphous alloys with diameters up to 5 mm have been synthesized by utilizing the high thermal stability of the supercooled liquid in Fe–(Co, Ni)–M–B (M = Zr, Hf, Nb, Ta, Mo, W) system.[6] Thermal properties of the Fe–(Co, Ni)–Zr–(Nb)–B amorphous alloys have been also investigated in a wide composition range.[7] They have found that the crystallization behavior changes from a single stage to two stages by the increase of Nb concentration more than 8 at%, leading to the decrease of ΔT_x. However, little is clear about the relationship between the formation of metastable phases at the primary stage of crystallization and the high stability of supercooled liquid in these complex alloy component systems.

In this study, we intend to examine the crystallization behavior of the simple three component $Fe_{90-X}Nb_{10}B_X$ (X = 10 and 30) system and discuss the origin for the high thermal stability of the amorphous Fe–Nb–B alloys with special attention to the atomic configurations of metastable crystalline and amorphous phases.

2. Experimental

Ternary $Fe_{80}Nb_{10}B_{10}$ and $Fe_{60}Nb_{10}B_{30}$ alloy ribbons were prepared by the single-roller melt spinning technique in an argon atmosphere. Their master ingots were prepared by arc melting the mixture of pure Fe and Nb metals and pure B crystal in an argon atmosphere. Thermal stability and phase transformation were investigated by differential scanning calorimetry (DSC) at a heating rate of 0.67 K/s. The amorphous samples were annealed at each annealing temperature (T_a) for 1200 s with a vacuum infrared furnace, and then cooled rapidly in the furnace. The heating rate of annealing was 0.67 K/s and the residual pressure of the furnace was kept to be less than 10^{-5} Pa during the experiment. The structures of the annealed samples were investigated by X-ray diffractmetry with Cu Kα radiation.

3. Results and Discussion

The thermal stability can be estimated by the supercooled liquid region, ΔT_x, defined by the difference between the glass transition temperature (T_g) and the onset temperature of crystallization (T_x). Figure 1 shows the DSC curves of the melt-spun amorphous $Fe_{80}Nb_{10}B_{10}$ and $Fe_{60}Nb_{10}B_{30}$ ribbons. In case of $Fe_{80}Nb_{10}B_{10}$, no glass transition is observed and the amorphous phase directly changes into crystalline phases upon heating. Three main exothermic peaks which correspond to the precipitation of crystalline phases are seen in this figure. On the other hand, the $Fe_{60}Nb_{10}B_{30}$ alloy exhibits the glass transition, followed by the appearance of a supercooled liquid. Two exothermic peaks with a temperature interval more than 100 K are seen. The values of T_x, T_g and ΔT_x for the $Fe_{80}Nb_{10}B_{10}$ and $Fe_{60}Nb_{10}B_{30}$ alloys are summarized in Table 1. It is important to point out that the increase in the boron content from 10 at% to 30 at% causes the significant change in the thermal behavior, *i.e.*, the appearance of the glass transition and large supercooled liquid region of $\Delta T_x = 67$ K.

The amorphous $Fe_{80}Nb_{10}B_{10}$ and $Fe_{60}Nb_{10}B_{30}$ alloys were

*Present address: *Alps Electric Co.*

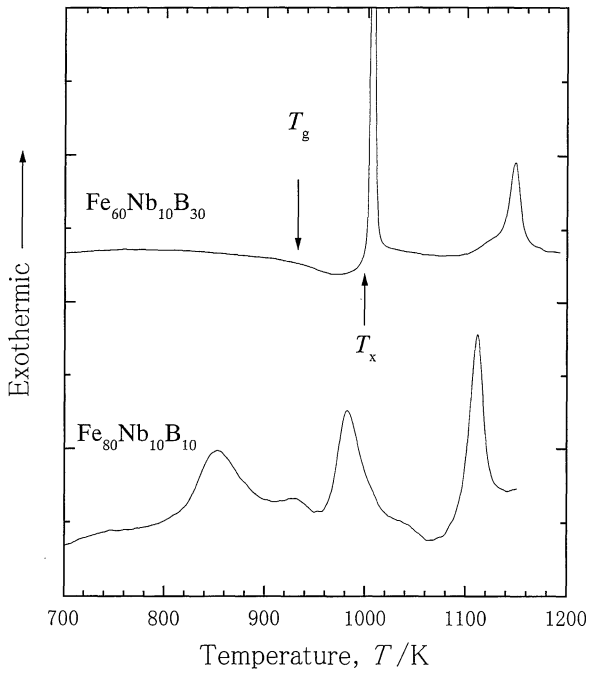

Fig. 1 DSC curves of $Fe_{80}Nb_{10}B_{10}$ and $Fe_{60}Nb_{10}B_{30}$ amorphous alloys.

Table 1 T_x, T_g and ΔT_x for $Fe_{80}Nb_{10}B_{10}$ and $Fe_{60}Nb_{10}B_{30}$ amorphous alloys.

	T_x/K	T_g/K	$\Delta T_x/K$
$Fe_{80}Nb_{10}B_{10}$	815	—	—
$Fe_{60}Nb_{10}B_{30}$	1001	934	67

Table 2 Annealing temperatures for $Fe_{80}Nb_{10}B_{10}$ and $Fe_{60}Nb_{10}B_{30}$ amorphous alloys.

	Metastable stage		Final stage
$Fe_{80}Nb_{10}B_{10}$	(1) 853 K	(2) 983 K	(3) 1273 K
$Fe_{60}Nb_{10}B_{30}$	(1) 940 K	(2) 1007 K	(3) 1273 K

annealed at several temperatures to investigate the crystallized phases of these alloys. The annealing temperatures are shown in Table 2. The $Fe_{80}Nb_{10}B_{10}$ alloy ribbons were annealed at 853 K and 983 K for 1200 s, which correspond to the first and second distinct exothermic peaks in the DSC curve, to obtain each metastable crystalline phase. The $Fe_{60}Nb_{10}B_{30}$ alloy was also annealed at 940 K and 1007 K for 1200 s in the same way. The structures of final crystalline phases were determined by X-ray analyses of the samples annealed at 1273 K for 1200 s for both alloys.

The X-ray diffraction patterns of the annealed $Fe_{80}Nb_{10}B_{10}$ samples are shown in Fig. 2. The patterns corresponding to the metastable crystalline phases annealed at 853 K and 983 K were identified to be isostructural with α-Mn type and α-Fe type phases, respectively. The α-Mn type structure has a body-centered symmetry and the lattice parameter is 0.8846 nm calculated by using the cell refinement module of JADE software (Materials Data Inc.). It is remarkable that the amorphous phase transformed into the primal single phase of

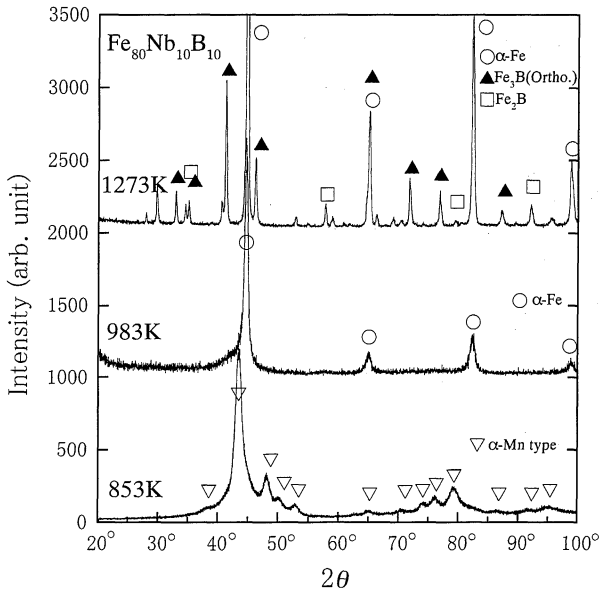

Fig. 2 X-ray diffraction patterns of the $Fe_{80}Nb_{10}B_{10}$ amorphous alloy annealed at 853 K, 983 K and 1273 K for 1200 s.

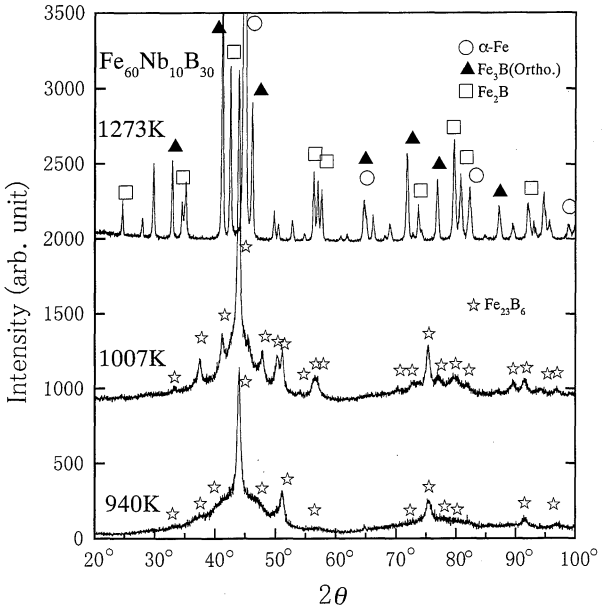

Fig. 3 X-ray diffraction patterns of the $Fe_{60}Nb_{10}B_{30}$ amorphous alloy annealed at 940 K, 1007 K and 1273 K for 1200 s.

α-Mn type and then, this phase directly changes into another single phase (α-Fe type). This suggests that the polymorphous reaction occurs in the primary crystallization process from the amorphous phase. The metastable α-Fe type phase changes into α-Fe, orthorhombic Fe_3B and Fe_2B at the final stage of crystallization. From these results, it is concluded that the crystallization of the $Fe_{80}Nb_{10}B_{10}$ alloy occurs as follows;

amorphous → α-Mn type → α-Fe type

→ α-Fe, Fe_3B (orthorhombic) and Fe_2B

The X-ray diffraction patterns of the annealed $Fe_{60}Nb_{10}B_{30}$ samples are shown in Fig. 3. In this case, the metastable

phase (annealed at 1007 K) is identified as a single phase of $Fe_{23}B_6$ type structure with a lattice parameter of 1.0735 nm. This phase has been reported in Fe–B binary system and is isostructural with $Cr_{23}C_6$ structure.[8] This phase seems to be partially formed in the supercooled liquid region by annealing at 940 K for 1200 s. The final crystalline phases are the same as those for the $Fe_{80}Nb_{10}B_{10}$ alloy and identified as α-Fe, orthorhombic Fe_3B and Fe_2B. Hence, the crystallization behavior of the $Fe_{60}Nb_{10}B_{30}$ alloy is summarized as follows;

$$\text{amorphous} \rightarrow \text{supercooled liquid} \rightarrow Fe_{23}B_6 \text{ type}$$
$$\rightarrow \alpha\text{-Fe},\ Fe_3B \text{ (orthorhombic) and } Fe_2B$$

To clarify the reason for the high thermal stability of the amorphous $Fe_{60}Nb_{10}B_{30}$ alloy, we tried to compare the local atomic configurations of the primary crystalline phase with those of amorphous phases.

In case of the $Fe_{80}Nb_{10}B_{10}$ alloy, the primary crystalline phase is identified as the α-Mn type structure. The same structure has been reported by Ohnuma *et al.*[9] They have showed the precipitation of α-Mn and/or β-Mn type phase in the crystallization process of $Fe_{80}P_{20-x}Si_x$ amorphous alloys and have pointed out that these structures consist of the Frank-Kasper coordination polyhedra, which are closely related to the local structure in these amorphous alloys. It seems important that the same structure is formed in the primary crystallization process of the Fe-based alloy containing the different metalloid element. Figure 4(a) shows a schematic drawing of 2 × 2 × 2 unit cells of the α-Mn type structure. All atom positions are shown by the sphere of the equal size for convenience because which element occupies which site is not clear up to the present. Anyway, there are four different sites in this structure and three types of Frank-Kasper structures can be considered in which all atoms have 12(icosahedral), 14 and 16 coordinations. In particular, the cell of the α-Mn type structure can be almost filled up with the icosahedral coordination polyherda. Some of them are also drawn in this figure. This type of polyhedron seems to be more or less expected in the Bernal type structure[10] of amorphous alloys, that would likely exist in the Fe–B systems containing less than 18 at%B.[11] Therefore, the phase transformation from the amorphous state to the crystalline state would occur easily with relatively short-range atomic diffusion.

The $Fe_{23}B_6$ type structure, which has a face-centered symmetry, is identified as the primary crystallization phase of the amorphous $Fe_{60}Nb_{10}B_{30}$ alloy. Figure 4(b) shows a schematic drawing of 2 × 2 × 2 unit cells of the $Fe_{23}B_6$ type structure. The positions of boron and metal atoms in this type of structure are represented by small and large spheres, respectively. In this structure, the cubo-octahedra and the cubes formed by metal atoms are connected with metalloid atom.[12] Thus, the boron atom is surrounded by eight metal atoms to form an Archimedean square antiprism. These Archimedean square antiprisms ought to be symmetrically arranged in the $Fe_{23}B_6$ structure. The configurations of the above-described polyhedra are also drawn in this figure. In the amorphous Fe–B alloys containing higher than 20 at%B, the local atomic structure is successfully characterized by the non-periodic network of the trigonal prisms.[13] This type of local ordering structure would be formed in the amorphous $Fe_{60}Nb_{10}B_{30}$ alloy because the boron concentration is higher than 20 at%. The coordination number around boron atom is expected to be 6 with the first nearest neighbors (and 3 with slightly further away positions) in these alloys. Therefore, the change in the chemical short-range order from the trigonal prism to the Archimedean square antiprism as well as the simultaneous arrangement of these polyhedra to form the $Fe_{23}B_6$ type symmetry should occur for the phase transformation from the amorphous phase to the primary crystalline phase.

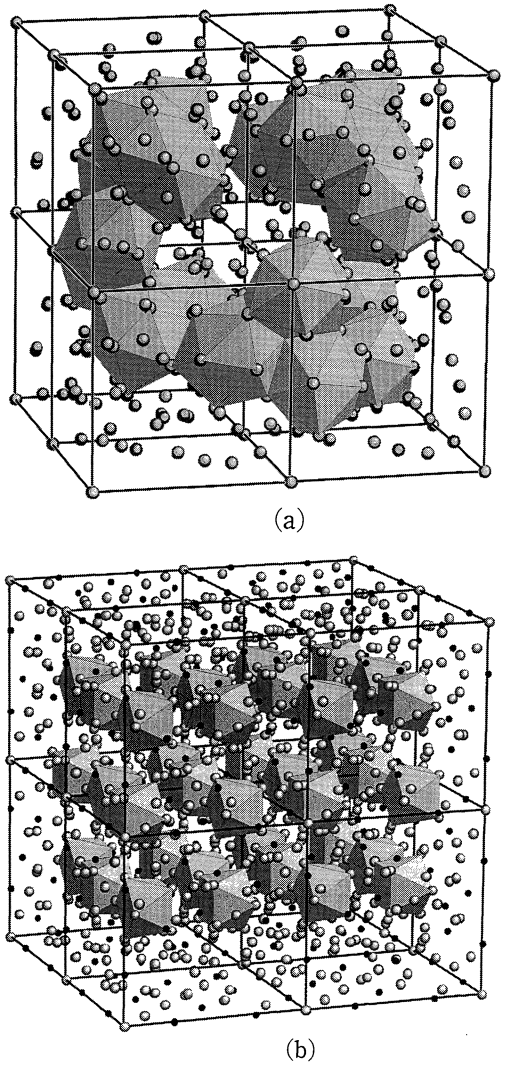

Fig. 4 Schematic drawings of 2 × 2 × 2 unit cells for (a) α-Mn type and (b) $Fe_{23}B_6$ type structures. (a) All atom positions are shown by the same spheres. (b) The positions of boron atoms are shown by smaller spheres. The icosahedral coordination polyhedra and the Archimedean square antiprism, are also drawn in the structures of (a) and (b), respectively.

The present results suggest that the high thermal stability of the amorphous $Fe_{60}Nb_{10}B_{30}$ alloy is attributed to the difficulty of the geometrical rearrangements in the relatively long-range ordering structures.

We have found that the some characteristic metastable phases are formed in the crystallization processes of $Fe_{80}Nb_{10}B_{10}$ and $Fe_{60}Nb_{10}B_{30}$ amorphous alloys. To advance the research on the mechanisms of the crystallization processes in these ternary alloys, it will be necessary to clarify

the redistribution behavior of composition in each crystallization stage.

4. Conclusions

A large supercooled liquid region, $\Delta T_x = 67$ K, appeared in the crystallization process of amorphous $Fe_{60}Nb_{10}B_{30}$ alloy, whereas the amorphous $Fe_{80}Nb_{10}B_{10}$ alloy directly transformed into crystalline phases. Two unique crystallization behaviors were found for these amorphous alloys, which are summarized as follows;

(1) In case of the $Fe_{80}Nb_{10}B_{10}$ alloy,

Amorphous $\rightarrow$ α-Mn type $\rightarrow$ α-Fe type

$\rightarrow$ α-Fe, Fe_3B (orthorhombic) and Fe_2B.

(2) In case of the $Fe_{60}Nb_{10}B_{30}$ alloy,

amorphous $\rightarrow$ supercooled liquid $\rightarrow$ $Fe_{23}B_6$ type

$\rightarrow$ α-Fe, Fe_3B (orthorhombic) and Fe_2B.

The precipitation of the $Fe_{23}B_6$ type structure requires a significant change in the local structure of the $Fe_{60}Nb_{10}B_{30}$ alloy, which may lead the high stability of the supercooled liquid before crystallization.

REFERENCES

1) A. Inoue, K. Ohtera, K. Kita and T. Masumoto: Jpn. J. Appl. Phys., **27** (1988), L2248–2251.
2) A. Inoue, H. Yamaguchi, T. Zhang and T. Masumoto: Mater. Trans., JIM, **31** (1990), 104–109.
3) A. Inoue, N. Nishiyama and H. Kimura: Mater. Trans., JIM, **38** (1997), 179–183.
4) A. Inoue, T. Zhang and T. Masumoto: Mater. Trans., JIM, **31** (1991), 1005–1010.
5) A. Inoue and J. S. Gook: Mater. Trans., JIM, **36** (1995), 1180–1183.
6) A. Inoue, T. Zhang and H. Koshiba: J. Appl. Phys., **83** (1998), 6326–6328.
7) A. Inoue, H. Koshiba, T. Zhang and A. Makino: Mater. Trans., JIM, **38** (1997), 577–582.
8) Y. Khan and H. Wibbeke: Z. Metallkde., **82** (1991), 703–705.
9) M. Ohnuma, O. Sasaki, H. Kuwano, S. Katano, Y. Morii, S. Funahashi, H. R. Child and Y. Hamaguchi: Mater. Trans., JIM, **34** (1993), 874–881.
10) J. D. Bernal: Nature, **183** (1959), 141–147.
11) Y. Waseda and H. S. Chen: Sci. Rep. Res. Inst. Tohoku Univ., **A28** (1981), 143–155.
12) *see for instance*, S. Nagakura and S. Oketani: Trans., ISIJ, **8** (1968), 202–231.
13) P. H. Gaskell: J. Non-Cryst. Solids, **32** (1979), 207–224.